

# Effects of the alkyl chain length in phosphonic acid self-assembled monolayer gate dielectrics on the performance and stability of low-voltage organic thin-film transistors

Kenjiro Fukuda,<sup>1</sup> Takanori Hamamoto,<sup>1</sup> Tomoyuki Yokota,<sup>1</sup> Tsuyoshi Sekitani,<sup>1</sup> Ute Zschieschang,<sup>2</sup> Hagen Klauk,<sup>2</sup> and Takao Someya<sup>1,a)</sup>

<sup>1</sup>Department of Electrical and Electronic Engineering and Department of Applied Physics, The University of Tokyo, 7-3-1 Hongo, Bunkyo-ku, Tokyo 113-8656, Japan

<sup>2</sup>Max Planck Institute for Solid State Research, Heisenbergstr. 1, 70569 Stuttgart, Germany

(Received 28 July 2009; accepted 9 October 2009; published online 16 November 2009)

We have fabricated pentacene organic thin-film transistors (TFTs) using self-assembled monolayers (SAMs) based on alkyl-phosphonic acids with five different alkyl chain lengths as the gate dielectric and investigated the relationship between the SAM chain length and the electrical performance and stability of the transistors. A SAM chain length of 14 carbon atoms provides a maximum TFT mobility of  $0.7 \text{ cm}^2/\text{V s}$ , along with an on/off current ratio greater than  $10^5$ . We have also investigated the bias stress effect in these TFTs and found that the change in drain current is substantially less severe than in pentacene TFTs with polymer gate dielectrics. © 2009 American Institute of Physics. [doi:10.1063/1.3259816]

Organic thin-film transistors (TFTs) are among the key elements for the realization of large-area, printable, and flexible electronics,<sup>1,2</sup> large-area sensors,<sup>3</sup> and actuators.<sup>4</sup> For these applications, it is desirable that the organic TFTs can be operated with voltages in the range of 1.5–2 V. TFTs with such low operating voltages require a gate dielectric with a large capacitance per unit area, such as a very thin insulating polymer,<sup>5,6</sup> a metal oxide with a large permittivity,<sup>7,8</sup> or a self-assembled nanodielectric.<sup>9,10</sup> While all of these high-capacitance dielectrics have been used to prepare individual low-voltage organic TFTs, so far none of them has been utilized for integrated circuits or other large-area applications based on low-voltage organic TFTs. In contrast, gate dielectrics based on an oxygen-plasma-grown  $\text{AlO}_x$  layer (with a thickness of a few nanometers) in combination with an alkyl-phosphonic acid self-assembled monolayer (SAM) have been employed to demonstrate not only low-voltage organic TFTs using a variety of organic semiconductors,<sup>11–13</sup> but also large-scale integrated circuits on flexible substrates with more than 100 organic TFTs.<sup>14</sup> All TFTs and circuits in these previous reports utilized the same SAM, n-octadecylphosphonic acid.

In this study, we have systematically investigated the relationship between the alkyl chain length of the phosphonic acid SAMs that form the gate dielectric and the electrical characteristics of the organic TFTs. Phosphonic acids with five different alkyl chain lengths [ $\text{CH}_3(\text{CH}_2)_{X-1}\text{PO}(\text{OH})_2$ ,  $X=6, 10, 14, 16,$  and  $18$ ] were selected and compared. The SAMs were prepared from solution. We have found that the TFT characteristics depend significantly on the chain length of the SAMs, and that n-tetradecylphosphonic acid ( $X=14$ , also referred to as C14-SAM in this study) provides the optimum performance. We have also investigated the dc bias stress effect in these TFTs and found that the bias stress-induced decrease in drain current is no more than 10% after

4000 s of continuous bias stress with a gate field of 2.5 MV/cm.

The cross section of the pentacene TFTs with the  $\text{AlO}_x/\text{SAM}$  gate dielectric is schematically shown in Fig. 1(a). First, a 25 nm thick Al gate electrode was thermally evaporated onto a silicon wafer through a shadow mask. The gate dielectric consists of a thin layer of aluminum oxide (5 nm thick) and a molecular alkyl-phosphonic acid SAM. The aluminum oxide film was prepared by oxygen-plasma treatment of the Al gate electrode and provides a large density of hydroxyl groups for molecular adsorption. The plasma power was 300 W, and the duration of the plasma treatment was 30 min. The SAM was prepared by submersing the substrate in a 2-propanol solution of the phosphonic acid molecules at room temperature. Five phosphonic acids with different alkyl chain lengths were studied which are as follows: n-hexyl (C6-SAM), n-decyl (C10-SAM),

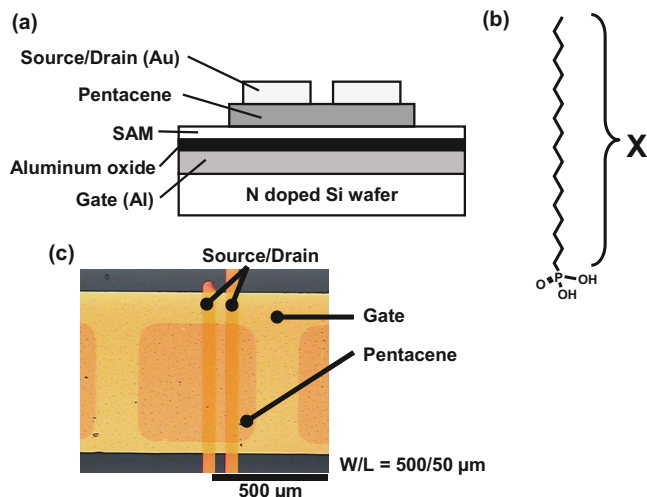


FIG. 1. (Color online) (a) Cross-section of the pentacene TFTs. The gate dielectric is a combination of a thin oxygen-plasma-grown aluminum oxide ( $\text{AlO}_x$ ) layer and a phosphonic acid SAM. (b) Chemical structure of n-octadecylphosphonic acid [ $\text{CH}_3(\text{CH}_2)_{X-1}\text{PO}(\text{OH})_2$ ,  $X=18$ ]. (c) Photograph of a pentacene TFT.

<sup>a)</sup>Author to whom correspondence should be addressed. Electronic mail: someya@ee.t.u-tokyo.ac.jp.

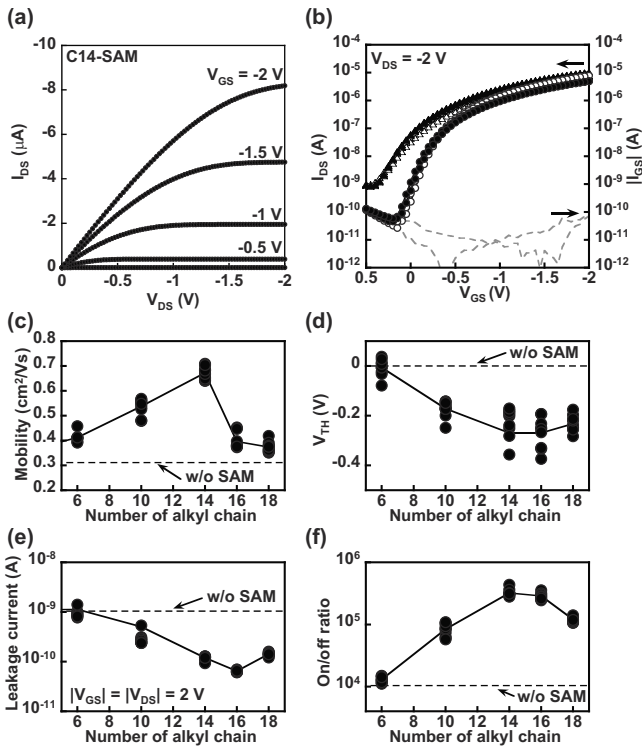


FIG. 2. Electrical TFT characteristics measured in ambient air at room temperature. (a) Output characteristics of a TFT with the C14-SAM ( $X=14$ ). (b) Transfer characteristics of TFTs with C18-SAM ( $X=18$ ), C14-SAM ( $X=14$ ), C6-SAM ( $X=6$ ), and without SAM (only 5 nm  $\text{AlO}_x$  as the gate dielectric). The dotted line is the gate current of the TFT with C14-SAM. (c) Carrier mobility, (d) threshold voltage, (e) gate current, and (f) on/off current ratio of TFTs with SAM. The dotted line in each graph represents the average parameter value obtained for the TFTs without any SAM (only 5 nm  $\text{AlO}_x$ ).

n-tetradecyl (C14-SAM), n-hexadecyl (C16-SAM), and n-octadecyl (C18-SAM) phosphonic acid [Fig. 1(b)]. Purified pentacene was vacuum deposited to form a 30 nm thick patterned semiconductor layer on the gate dielectric. Finally, 50 nm thick Au was evaporated to form source and drain contacts. For comparison, we also fabricated pentacene TFTs with only the 5 nm thick aluminum oxide as a gate dielectric (without any SAM). The nominal channel length and channel width were 50 and 500  $\mu\text{m}$  for all TFTs.

The dc characteristics of the TFTs were measured in ambient air at room temperature using a semiconductor parameter analyzer (4155C, Agilent Technologies). Figure 2(a) shows the output characteristics of a TFT with the C14-SAM as the gate dielectric. The drain current ( $I_D$ ) was measured as a function of the drain-source voltage ( $V_{DS}$ ) for gate-source voltages ( $V_{GS}$ ) from 0 to  $-2$  V in steps of 0.5 V. Figure 2(b) shows the transfer characteristics of TFTs with C18-SAM, C14-SAM, C6-SAM, and without any SAM. From the electrical TFT characteristics, the parameters carrier mobility in the saturation regime, threshold voltage, gate current, and on/off current ratio were extracted. Figures 2(c)–2(f) show how these parameters depend on the alkyl chain length of the phosphonic acid molecules. The dotted line in each graph represents the average parameter value obtained for the TFTs without any SAM. Figure 2(c) shows that increasing the alkyl chain length from 6 to 14 carbon atoms causes the mobility to increase from 0.4 to 0.7  $\text{cm}^2/\text{V s}$ , while further increasing the chain length to 18 carbon atoms causes the mobility to drop to 0.4  $\text{cm}^2/\text{V s}$  again. The mobility of the

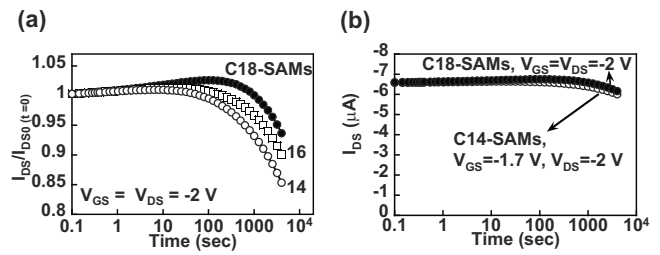


FIG. 3. Time-dependent drain current during continuous DC bias stress. (a) TFTs with C14-SAM, C16-SAM and C18-SAM stressed with  $V_{GS}=V_{DS}=-2$  V. The drain current has been normalized to the initial value at  $t=0$  s. (b) A TFT with C18-SAM stressed with  $V_{GS}=V_{DS}=-2$  V, and a TFT with C14-SAM stressed with  $V_{GS}=-1.7$  V and  $V_{DS}=-2$  V. These bias conditions give a similar electric field across the gate dielectric and the same initial drain current for both TFTs (6.5  $\mu\text{A}$ ).

TFTs without SAM (only  $\text{AlO}_x$ ) is only 0.3  $\text{cm}^2/\text{V s}$  and therefore smaller than the mobility of any of the TFTs with SAM dielectric. Figure 2(d) shows that the threshold voltage increases from 0 V for TFTs with C6-SAM to about  $-0.2$  V for TFTs with longer chain length. This relationship between gate dielectric thickness and threshold voltage is similar to that observed in silicon field-effect TFTs with very thin inorganic oxide gate dielectrics.<sup>15</sup>

The greatest concern with thin gate dielectrics is the undesirable charge leakage through the dielectric. Figure 2(e) shows that the gate current in the TFTs with C6-SAM is approximately the same as that in TFTs without any SAM, about 1 nA. As the alkyl chain length is increased to 16 carbon atoms, the gate current decreases monotonically to below 100 pA. This confirms the important role of a well-ordered SAM in providing a gate dielectric with low leakage currents. The leakage through the gate dielectric also sets a lower limit to the minimum off-state drain current and therefore to the on/off current ratio of the TFTs. As shown in Fig. 2(f), the on/off ratio improves from  $10^4$  for TFTs with C6-SAM to above  $10^5$  for TFTs with C14- and C16-SAM. The minimum gate current is 60 pA for the TFTs with C16-SAM, and the maximum on/off ratio is  $4 \times 10^5$  for the TFTs with C14-SAM.

We have also investigated the dc bias stress effect of fabricated TFTs with various SAM gate dielectrics.<sup>16,17</sup> Figure 3(a) shows how the drain current of TFTs with C14-, C16-, and C18-SAM changes over time while the TFTs are being stressed with constant voltages ( $V_{GS}=V_{DS}=-2$  V). The drain currents in Fig. 3(a) have been normalized to their initial values. The drain current increased slightly for first 100 s. This may be due to the threshold shift originated from atmospheric components  $\text{O}_2$  and/or  $\text{H}_2\text{O}$  adsorbed to the pentacene and plastic substrates.<sup>18,19</sup> When dc bias voltages of  $-2$  V were applied to the SAM-dielectric TFTs continuously for 4000 s, the drain current decreased to 93% of the initial value in the TFT with C18-SAM and to 85% of the initial value in the TFT with C14-SAM. In this experiment, the threshold voltage of the TFTs with shorter SAM chain length shifts more rapidly, because a shorter SAM implies a thinner gate dielectric and hence a larger electric field. We have also compared the bias stress-induced time-dependent change in drain current of two TFTs with different SAMs under bias conditions that provide similar electric field and exactly the same initial drain current [Fig. 3(b)]. After stressing the TFTs continuously for 4000 s under these bias conditions, the drain current of the TFT with the C18-SAM de-

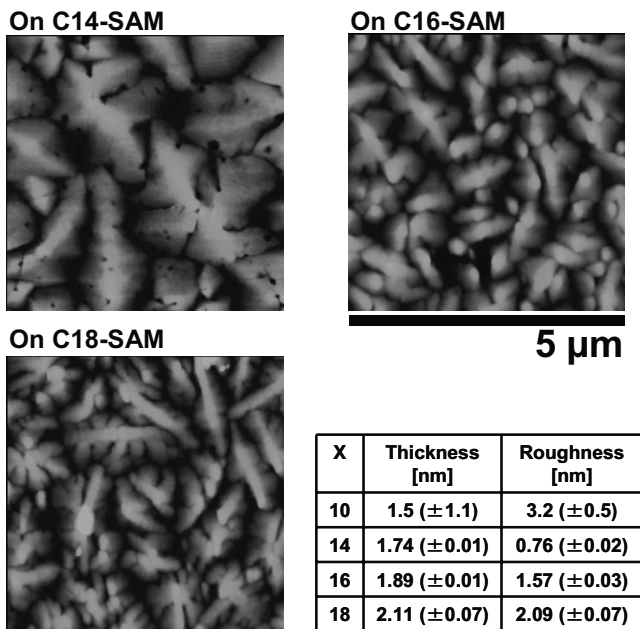


FIG. 4. Pentacene morphology observed with an atomic force microscope. The scan size is  $5 \times 5 \mu\text{m}^2$ . The inset table shows the thickness and surface roughness of the C10-SAM, C14-SAM, the C16-SAM, and the C18-SAM obtained by fitting of the x-ray reflectivity data.

creased from 6.6 to 6.2  $\mu\text{A}$ , and the drain current of the TFT with the C14-SAM decreased from 6.6 to 6.0  $\mu\text{A}$ . This decrease in drain current is significantly smaller than in pentacene TFTs with polymer gate dielectrics.<sup>20</sup>

In order to better understand the nonmonotonic relationship between the alkyl chain length of the SAM employed for the gate dielectric and the carrier mobility of the pentacene TFTs [Fig. 2(c)], we have evaluated the thin-film morphology of the pentacene films by atomic force microscopy and the surface roughness of the various SAMs by x-ray reflectivity. Figure 4 shows the surface morphology of the pentacene films on the C14-, C16-, and C18-SAM. On the C14-SAM the pentacene has a grain size of approximately 3  $\mu\text{m}$ , which is notably larger than on the C16- and C18-SAMs. The inset in Fig. 4 gives the thickness and the surface roughness of the C10-, C14-, C16-, and C18-SAM, which were obtained by fitting of the measured x-ray reflectivity curves. According to these data, the C10-SAM does not form flat monolayer on the  $\text{AlO}_x$ , and C14-SAM is substantially smoother than the C16-SAM and the C18-SAM, which may explain the larger grain size and the larger mobility of the pentacene films on the C14-SAM. The difference in surface roughness between phosphonic acid SAMs with different alkyl chain lengths may be related to subtle differences in the packing density and the conformation of the alkyl chains within the SAM, depending on the chain length.<sup>21</sup>

The relationship between the alkyl chain length and the microscopic SAM structure has been studied for a number of molecule/substrate combinations, such as carboxylic acid SAMs on aluminum oxide<sup>22</sup> and phosphonic acid SAMs on silicon oxide,<sup>23</sup> but there are no reports on the relationship between the alkyl chain length and the SAM structure of phosphonic acids on aluminum oxide. As Tao<sup>22</sup> have pointed out, the SAM microstructure is very sensitive to the exact binding mechanism, and is therefore expected to be different for each system. Therefore, we can only speculate that alkyl-phosphonic acids with a chain length of less than about ten

carbon atoms form mostly disordered, liquidlike monolayers, possibly due to a lack of cohesive interaction between the molecules.<sup>21,22</sup> This would explain the large gate currents of the TFTs with the C6-SAM. For molecules longer than about ten carbon atoms, the cohesive forces are expected to be sufficiently strong to force the molecules into an almost upright position with an all-trans zigzag conformation, yielding dense, well-ordered monolayers with a very smooth surface<sup>22</sup> that provides for optimum pentacene film growth, explaining the excellent performance of the TFTs with C14-SAM. Our observation that the C16-SAM and C18-SAM have a larger surface roughness than the C14-SAM may indicate a larger density of gauche defects near the top surface of the monolayer when the chain length exceeds about 14 carbon atoms.<sup>24</sup>

This study was partially supported by WAKATE S, NEDO, Special Coordination Funds for Promoting Science and Technology, and Global COE Program on Physical Sciences Frontier, MEXT Grant No. 20676005.

<sup>1</sup>J. A. Rogers, Z. Bao, K. Baldwin, A. Dodabarapur, B. Crone, V. R. Raju, V. Kuck, H. Katz, K. Amundson, J. Ewing, and P. Drzaic, *Proc. Natl. Acad. Sci. U.S.A.* **98**, 4835 (2001).

<sup>2</sup>T. Sekitani, H. Nakajima, H. Maeda, T. Fukushima, T. Aida, K. Hata, and T. Someya, *Nature Mater.* **8**, 494 (2009).

<sup>3</sup>T. Someya, Y. Kato, T. Sekitani, S. Iba, Y. Noguchi, Y. Murase, H. Kawaguchi, and T. Sakurai, *Proc. Natl. Acad. Sci. U.S.A.* **102**, 12321 (2005).

<sup>4</sup>Y. Kato, T. Sekitani, M. Takamiya, M. Doi, K. Asaka, T. Sakurai, and T. Someya, *IEEE Trans. Electron Devices* **54**, 202 (2007).

<sup>5</sup>M. H. Yoon, H. Yan, A. Facchetti, and T. J. Marks, *J. Am. Chem. Soc.* **127**, 10388 (2005).

<sup>6</sup>S. Y. Yang, S. H. Kim, K. Shin, H. Jeon, and C. E. Park, *Appl. Phys. Lett.* **88**, 173507 (2006).

<sup>7</sup>J. B. Koo, S. J. Yun, J. W. Lim, S. H. Kim, C. H. Ku, S. C. Lim, J. H. Lee, and T. Zyung, *Appl. Phys. Lett.* **89**, 033511 (2006).

<sup>8</sup>M. F. Chang, P. T. Lee, S. P. McAlister, and A. Chin, *IEEE Electron Device Lett.* **29**, 215 (2008).

<sup>9</sup>M. H. Yoon, A. Facchetti, and T. J. Marks, *Proc. Natl. Acad. Sci. U.S.A.* **102**, 4678 (2005).

<sup>10</sup>S. A. DiBenedetto, D. Frattarelli, M. A. Ratner, A. Facchetti, and T. J. Marks, *J. Am. Chem. Soc.* **130**, 7528 (2008).

<sup>11</sup>H. Klauk, U. Zschieschang, J. Pflaum, and M. Halik, *Nature (London)* **445**, 745 (2007).

<sup>12</sup>H. Klauk, U. Zschieschang, R. T. Weitz, H. Meng, F. Sun, G. Nunes, D. E. Keys, C. R. Fincher, and Z. Xiang, *Adv. Mater.* **19**, 3882 (2007).

<sup>13</sup>P. H. Wöbkenberg, J. Ball, F. B. Kooistra, J. C. Hummelen, D. M. deLeeuw, D. D. C. Bradley, and T. D. Anthopoulos, *Appl. Phys. Lett.* **93**, 013303 (2008).

<sup>14</sup>K. Ishida, N. Masunaga, Z. Zhou, T. Yasufuku, T. Sekitani, U. Zschieschang, H. Klauk, M. Takamiya, T. Someya, and T. Sakurai, *IEEE J. Solid State Circuits*, 2009 (unpublished).

<sup>15</sup>J. K. Schaeffer, D. C. Gilmer, S. Samavedam, M. Raymond, A. Haggag, S. Kalpat, B. Steimle, C. Capasso, and B. E. White, Jr., *J. Appl. Phys.* **102**, 074511 (2007).

<sup>16</sup>R. Libsch and J. Kanicki, *Appl. Phys. Lett.* **62**, 1286 (1993).

<sup>17</sup>U. Zschieschang, R. T. Weitz, K. Kern, and H. Klauk, *Appl. Phys. A: Mater. Sci. Process.* **95**, 139 (2009).

<sup>18</sup>K. Fukuda, T. Sekitani, and T. Someya, *Appl. Phys. Lett.* **95**, 023302 (2009).

<sup>19</sup>D. Kumaki, M. Yahiro, Y. Inoue, and S. Tokito, *Appl. Phys. Lett.* **90**, 133511 (2007).

<sup>20</sup>D. Kawakami, Y. Yasutake, H. Nishizawa, and Y. Majima, *Jpn. J. Appl. Phys., Part 2* **45**, L1127 (2006).

<sup>21</sup>D. M. Spori, V. N. Venkataraman, S. G. P. Tosatti, F. Durmaz, N. D. Spencer, and S. Zürcher, *Langmuir* **23**, 8053 (2007).

<sup>22</sup>Y. T. Tao, *J. Am. Chem. Soc.* **115**, 4350 (1993).

<sup>23</sup>I. G. Hill, C. M. Weinert, L. Kreplak, and B. P. van Zyl, *Appl. Phys. A: Mater. Sci. Process.* **95**, 81 (2009).

<sup>24</sup>L. Motte and M. P. Pileni, *Appl. Surf. Sci.* **164**, 60 (2000).